Gas Sorption in Polyaniline. 1. Emeraldine Base

John Pellegrino* and Ray Radebaugh

National Institute of Standards and Technology, Physical and Chemical Properties Division, 838.01 and 838.09, 325 Broadway, Boulder, Colorado 80303

Benjamin R. Mattes

Los Alamos National Laboratory, CST-6, MS-J963, Los Alamos, New Mexico 87575

Received September 7, 1995[⊗]

ABSTRACT: Measurements of the sorption isotherms (at 298 K) for Ar, O_2, and N_2 in several polyaniline emeraldine base (PANi-EB) forms were made (as-cast film, powder, and fully undoped film) over the pressure range 100−1300 kPa. Model fits of the sorption isotherms were made using a modified Flory−Huggins equation (MFHE) and a dual mode sorption equation. In general, the variation of parameters for the MFHE was consistent with morphological interpretations from prior X-ray scattering studies. The ordering of gas sorption with respect to a particular PANi-EB form correlates with the relative sizes and condensabilities of the gas molecules. We see evidence that the morphological variations between different PANi-EB forms, as indicated by their He densities and X-ray scattering data, affects the ratio of O_2/N_2 solubilities primarily through restricted access to available free volume. From our current measurements of solubilities and prior results for the O_2 and N_2 permeabilities, we conclude that the O_2/N_2 ideal separation factor is due to diffusivity selectivity in an as-cast PANi-EB film and solubility selectivity in a fully undoped one.

Introduction

In this paper we present sorption data for Ar, O_2, and N_2 in the polyaniline emeraldine base (PANi-EB) polymer. Measurements were made on films and a powder in order to identify any significant film-processing-induced effects. A modified Flory−Huggins model, following Bitter,[1] was used to correlate the data in terms of two parameters. These parameters can be based (to a limited degree) on other fundamental properties, e.g., partial molar volumes and interaction potentials, rather than being purely empirical correlations. The sorption data and physical interpretation of the solubility model parameters are discussed further using structural insights provided by X-ray scattering results from Maron et al.[2]

During the late 1980s, a great deal of research was devoted to studies of the gas transport phenomena through membranes prepared with the π-conjugated polymer poly(trimethylsilylpropyne) (PTMSP).[3] This glassy polymer is remarkable since gas permeabilities through PTMSP films are the highest known for any polymer system; however, the gas selectivities are poor for most important separations. At the beginning of this decade, other classes of conjugated polymers were investigated for gas separations such as polyaniline[4−6] [PANi], poly(dimethoxy-*p*-phenylenevinylene)[4] [DMP-PV], and poly(*N*-methylpyrrole)[7] [PPY]. Unlike PTMSP, these other conjugated polymer systems are low in intrinsic gas permeability but exhibit very high selectivities, especially polyaniline. These highly selective conjugated membranes are achieved through a post-membrane formation procedure that involves a chemical modification process called "doping". Once exposed to either an oxidizing or a reducing agent (or, in the special case of the emeraldine base form of polyaniline, to an acid), the polymer becomes electrically conducting. In terms of gas transport properties, it is noteworthy that the family of π-conjugated polymers, known as "conducting polymers", presents the highest ideal separation factors.

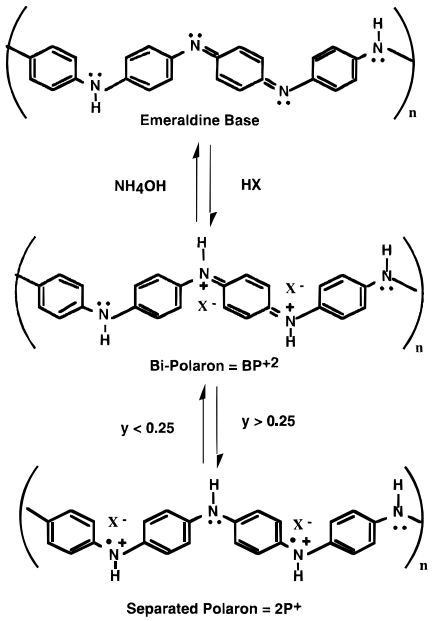

Figure 1. Polyaniline (PANi) emeraldine form. Neutral base form (top) is shown along with reversible protonic doping and undoping with a halogenic acid to bipolaron (middle) and separated polaron (bottom). y is the ratio of X^- to total N with $y = 0.5$ the fully doped state.

Polyaniline. The emeraldine oxidation state (Figure 1) of polyaniline is stable under ambient atmospheric conditions. Some of its physical−chemical properties such as electrical conductivity can be tailored by acid−base chemistry. Treating the emeraldine base (EB) with protonic acids is the "doping" process and yields emeraldine salts (ES). The electrical conductivity varies from $<10^{-10}$ (the insulating EB form) to >10 S/cm (for the fully doped ES form) by varying the amount of acid added to the EB form. For comparison, copper has a conductivity of approximately 10^6 S/cm. Figure 1 presents the changes in the monomer repeat unit as the acid−base chemistry is performed on PANi.

* To whom correspondence should be addressed.
[⊗] Abstract published in *Advance ACS Abstracts,* June 1, 1996.

S0024-9297(95)01333-7

A number of reports[4−6] on measurements of pure gas permeabilities through forms of PANi films have suggested their usefulness for membrane-based gas separations. These studies have reported a number of effects on pure gas permeabilities resulting from treatments of the PANi-EB film. These include the following:

(i) The permeability of selected gases (He, H_2, CO_2, O_2, Ar, N_2, and CH_4) through "as-cast" PANi-EB films essentially follows a size-dependent (kinetic diameter) relationship.

(ii) Changing the film from the as-cast EB form to a fully doped (FD) ES form with halogenic acids causes a decrease in gas permeabilities. This decrease depends on both the particular gaseous solute and the halogenic acid.

(iii) Undoping the PANi-ES/FD film (by addition of NH_4OH) back to the EB form yields an "undoped" or "cycled" EB film. The gas permeabilities in these films are uniformly larger than in the original as-cast films. Additionally, the ratio between the pure gas permeabilities for various gas pairs (the ideal separation factor) decreased in the undoped films relative to either the as-cast or FD-ES forms.

(iv) The permeability of any gas in the undoped EB film varied with the halogenic acid used to dope it. A clear trend of decreasing permeability, $F^- > Cl^- > Br^- > I^-$, as the acid anion changed followed the size order of the solvated halogen ion and was opposite the normal order of the counterion size in a crystal lattice.

(v) Reexposing an undoped film to a halogenic acid (called redoping) can be used to further modify a pure gas component's permeability through the resulting film. An optimum in the ideal separation factor for several gas pairs, including O_2/N_2 and H_2/N_2, with respect to the amount of redoping has been reported.[6,8]

The permeability of gases in polymers is determined by both their diffusion coefficient and their equilibrium solubility. The solubility, as a thermodynamic quantity, will be dependent on both structural parameters and chemical interactions between the solute and the polymer. A quantitative description of the thermodynamics of gas sorption in a polymer is integral to optimizing its development and use in membrane-based gas separations, sorbent processes, and barrier applications.

Experimental Section

Materials. Aniline ($C_6H_5NH_2$) was fractionally distilled in vacuo over barium oxide (0.67 kPa, boiling point range 346−355 K). Ammonium peroxydisulfate ($(NH_4)_2S_2O_8$), 1-methyl-2-pyrrolidinone [(NMP), $(CH_3)NC_4H_6O$], and pyrrolidine (C_4H_9N) were used as purchased (ACS Reagent Grade). Ammonium hydroxide, 29% (mass/mass) [NH_4OH], was used as purchased (ACS Reagent Grade). Tetrahydrofuran (THF) [C_4H_4O] was dried with sodium and benzophenone as an indicator and vacuum distilled prior to use. Hydrochloric acid (HCl) (38% mass/mass) was used as purchased (ACS Reagent Grade).

Synthesis of Polyaniline Powder in the Emeraldine Oxidation State. A solution 1 N in HCl was prepared by adding 491.7 g of concentrated HCl to a 5 L volumetric flask and then filling to the mark with distilled deionized water. A 425 mL aliquot of this acid solution was placed into a 3000 mL polymerization vessel along with 122.7 g (1.32 mol) of distilled aniline and maintained with stirring at 276 K. A 575 mL aliquot of 1 M HCl was combined with 69.03 g (0.303 mol) of ammonium peroxydisulfate in a separate flask. This mixture was stirred until all of the oxidant dissolved and then cooled to 273 K in a freezer. The persulfate solution was slowly added dropwise to the aniline solution by means of an addition funnel over the course of 60 min. The combined solutions reacted for an additional 3.5 h. The green emeraldine hydrochloride precipitate was collected on filter paper in a large Büchner funnel. The powder was extracted first with water and then with methanol, until the wash solutions were colorless, and then refiltered. This as-synthesized polyemeraldine hydrochloride salt was subsequently immersed in 5 L of 0.1 M NH_4OH for 3 h, filtered, and then washed once again with THF and methanol until the solutions were clear. The yield was calculated at 24%. The purified emeraldine base was vacuum-dried ($<1.4 \times 10^{-3}$ Pa) and stored in a vacuum dessiccator for further use. Four-point probe dc conductivity measurements of a vacuum-dried and -pressed EB powder (after immersion in 4 M HCl for 48 h to form the fully doped ES) yielded 1.2 S/cm.

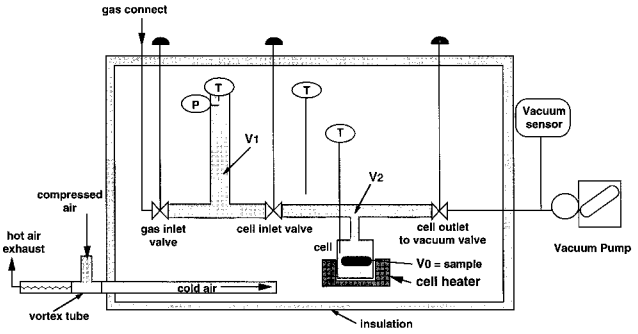

Figure 2. Schematic of apparatus to measure gas sorption by the pressure decay technique. Thermal environment is a convection oven. General air circulation and temperature control from rotary fan and fin heater. V_1 is the volume of the reservoir, and V_2 is the volume associated with a cell containing the sample of volume V_0. Vortex tube provides a steady stream of chilled air, and separate heating of the cell and sample can be controlled by an additional heater/controller.

Preparation of Emeraldine Base Films. A 2.0 g sample of EB powder was ground to a fine powder with a mortar and pestle. The powder was added incrementally to a mixture of 16 mL of NMP and 0.6 mL of pyrrolidine. The solution was covered and placed in an oven at 333 K for 30 min. The resulting homogeneous solution was free of particles, and it remained stable without gelation for weeks. Films were formed on glass plates by means of a gardner blade and annealed at 398 K for 3 h with an oven purge stream of argon gas. The as-cast films were removed from the plates by immersing them in a distilled water bath. They were extracted in methanol for 48 h to remove residual casting solvent. The as-cast emeraldine base films were immersed in 4 M HCl for 48 h to give a fully doped membrane. The fully doped films were immersed in a 0.1 M NH_4OH solution for 48 h to give the undoped (or cycled) film. The film was dried under vacuum ($<1.4 \times 10^{-3}$ Pa) for 48 h after each chemical treatment.

Apparatus. Two dual-volume, pressure-decay, sorption apparatus[9,10] were used for these studies: (1) a convection oven temperature control system that used a single pressure transducer and (2) a water bath temperature control system with two pressure transducers. The convection oven system is shown schematically in Figure 2. The water bath system was similar except that it had a second pressure transducer on the sample cell volume, and the whole apparatus was immersed in a water bath fed by a commercial, circulating-water temperature controller.

The convection oven system was designed to allow relatively rapid temperature changes. It also had smaller gas reservoir and sample cell volumes that facilitated the use of small sample sizes. A vortex cooler was used to maintain a steady supply of cool air, and the oven's two heaters and temperature controllers (one on the sample cell and the other on the circulation fan) maintained the oven temperature ±0.5 K. The temperatures in the sample cell, in the reservoir volume, and in the external oven volume were measured with Type K thermocouples. The valves were of an all-metal welded-bellows type, and the pressure transducer was a four-arm strain gage embedded in silicon crystal. The transducer had a range of 0−2068 kPa (0−300 psia) with an accuracy of ±2 kPa and a resolution (repeatability) of ±0.2 kPa. Calibration and resolution were verified and maintained by using a

portable pressure standard with 0.7 kPa accuracy and 0.007 kPa resolution. The measured volumes of the reservoir and sample cell were 3.311 and 2.900 cm^3, respectively.

The water bath system maintained better temperature stability and could accommodate an overall larger apparatus and sample cell volume. The temperature stability was ±0.2 K. The two pressure transducers used in this apparatus use variable capacitance designs. The transducers had a range of 0−1724 kPa (0−250 psia) with an accuracy of 1.9 kPa and a resolution (repeatability) of 0.3 kPa. In this system the temperature was measured in both the reservoir and sample cell volumes with Type T thermocouples. The measured volumes of the reservoir and sample cell were 35.398 and 9.743 cm^3, respectively.

The real-time temperature and pressure measurements in the sample cell and reservoir volume were used to calculate the gases' densities (and fugacities) with the 32-term modified Benedict−Webb−Rubin (MWBR) equation of state and tabulated parameters for each gas.[11,12] The gas densities, the absolute volumes of the reservoir and the sample cell, and the sample volumes were used to determine the mass balance and the amount of gas sorbed by the sample.

The volumes of the reservoir (V_1) and the sample cell (V_2) were determined using He as the calibration gas and a pure copper disk(s) of known volume (V_0). The calibration procedure involved two steps: First, the pressure was measured with volume V_1 pressurized and isolated from the evacuated volume V_2, and then it was measured again after V_2 was connected to V_1. Several sequences of these initial and final pressure measurements were made. The gas densities were calculated for each measurement, and the final density was plotted versus the initial value. The slope was proportional to $V_1/(V_1 + V_2)$. Second, the copper disk was inserted in volume V_2, and the above procedure was repeated. In this case the slope was proportional to $V_1/(V_1 + V_2 - V_0)$.

After initial volume calibrations a different standard-volume copper disk ($V_0 = 0.6287$ cm^3) was inserted as a check. Its volume was measured to be 0.6282 cm^3. This agreement for a single volume measurement was well within our estimated uncertainty for measuring the sample volumes (V_s). By using a propagation of uncertainties calculation, we estimated the standard deviation on V_s to be ±0.011−0.02 cm^3. This will depend on the volume of the actual sample and the volume of the calibration disk(s).

Helium was used to determine the volume of the actual experimental samples by monitoring the pressure decay in the sample cell until steady state was reached. This is essentially the same procedure that was used to determine the apparatus volumes and for measuring solute sorption. The assumption is that He does not have specific interactions with the polymer and provides a measure of its true volume. The mass of the sample was determined after degassing at high vacuum ($\sim 10^{-4}$ Pa) and weighing under vacuum ($\sim 10^{-2}$ Pa). The combination of the sample's mass and volume provides its density.

Uncertainty Estimate for Solubility Data. The uncertainty limits on the solubility data have been estimated to vary between ±7 and ±18% of the reported value based on maximum instrumental and calibration uncertainties. The uncertainty based on reproducibility of individual data points (where available) and the variance in the average pressure and temperature data used in calculating the molar sorption was ±1 to ±10% of the reported value.

Modeling

Measurement of the glass transition temperature (T_g) of the EB material, using DMTA, yielded a value of 523 K. This is in the same range as the value of 473 K reported by Wei et al.[13] Both values are well above the 298 K where our sorption measurements were made, so we can consider PANi a glassy polymer and apply the theoretical frameworks typically used in that case. Using our experimental isotherms, we calculated parameters for two models: modified Flory−Huggins and dual-mode sorption and the single-parameter linear fit (forced through the origin) for the solubility coefficient, $S = C/f$. The sorption model based on a modified Flory−Huggins equation (MFHE), presented by Bitter,[1] was chosen as the primary context in which to evaluate the experimental results. This model is similar in form to the gas−polymer−matrix model of Raucher and Sefcik,[14] which assumes that all gas molecules in the glassy polymer exist as a single population and that the observed nonlinearities in isotherms are due to gas−polymer interactions.

The MFHE model (eq 1) has contributions from athermal entropic processes (the first three bracketed terms on the right side) and a contribution from the heat of mixing. This model assumes that all sorption occurs in the noncrystalline (amorphous) volume of the polymer. It is derived in general form for multiple solutes and is not limited to a glassy polymer. The entropic contribution includes the effect of elastic strain (the third bracketed term on the right side), which may be fairly significant in a glassy polymer. According to the MFHE model, the activity a_i of each penetrant is given by

$$\ln(a_i) = \left[\ln\left(\frac{Z_i}{Z_{av}}\Phi_i\right)\right] + \left[1 - \frac{V_i Z_i}{V_{av} Z_{av}}\Phi_s\right] + \left[\frac{V_i}{C_L}\Phi_a^{2/3}\right] + \left[\frac{\Delta H_i^{mix}}{RT}\right] \quad (1)$$

The Φ are volume fractions (Φ_i = volume fraction of solute in the amorphous region of the polymer, Φ_s = volume fraction of all permeants in the amorphous fraction of the polymer, and Φ_a = volume fraction of polymer in the swollen amorphous phase). The Z are coordination numbers in the hypothetical lattice in the polymer (Z_i = coordination number of pure component i and Z_{av} = average coordination number of the swollen polymer phase). C_L is the elastic strain parameter. C_L is a function of the partial molar volume of polymer segments and other quantities that reflect the degree of strain resulting from rearrangement of the amorphous polymer. V_i is the partial molar volume of component i, and V_{av} is the average partial molar volume of all penetrants. The partial molar enthalpy of mixing of component i with the polymer is ΔH_i^{mix}.

At low gas concentrations in the polymer phase, Bitter proposed simplifications to eq 1 that give rise to a relationship between the equilibrium concentration of permeant in the polymer C_i (cm^3 [STP][15] of gas per cm^3 of polymer) and its gas phase fugacity, f_i:

$$C_i = \frac{{}^{\infty}H_i f_i}{1 - \Phi_s} \exp(B_i \Phi_s) \quad (2)$$

Equation 2 has two main parameters: (1) ${}^{\infty}H_i$, the Henry's parameter at infinite dilution, and (2) B_i, which expresses the nonideal behavior of the polymer−gas mixture. For a single component $\Phi_s = \Phi_i = V_i C_i \phi_a^{-1} c^{-1}$, where ϕ_a is the volume fraction of polymer in the amorphous phase (before sorption) and c = cm^3/mol of gas at STP (for an ideal gas c = 22.4 L/mol). Equation 2 is nonlinear due to the presence of C_i in the expression for Φ_s (or Φ_i) that appears in the exponent on the right-hand side and must be solved numerically.

In eq 2 the gas−polymer interaction parameter B_i is defined by

$$B_i = \frac{V_i}{9v}\frac{2f(s)-1}{f(s)^2} + 2\frac{V_i}{RT}\delta_{ip}{}^2 + \frac{V_i}{V_{av}}\frac{Z_i}{Z_{av}} \qquad (3)$$

where $\delta_{ip}{}^2$ is the binary mixture parameter, v is the partial molar volume of the polymer segments, and $f(s)$ is related to the induction of strain. The first term in the brackets can take on a variety of values depending on the swelling-induced strain in the polymer. In discussing the significance of B_i, Bitter describes the relative contribution from elastic strain such that, in a rubbery polymer, the amorphous polymer chains can easily rearrange to accommodate the volume of penetrants. In glassy polymers, penetrants introduce more strain, which increases the overall activity of the solute in the polymer. B_i can be both positive (in rubbery materials) and highly negative (in glassy polymers). In general, the more negative B_i is, the greater the strain that is introduced by the sorbing penetrant.

The effects of temperature and changes in the chemical interactions are mostly reflected in ${}^{\infty}H_i$, the Henry's parameter at infinite dilution, described by

$${}^{\infty}H_i = \frac{K_H}{f_{sat,i}}\exp\left(-\frac{V_i}{RT}\delta_{ip}{}^2\right) \qquad (4)$$

where $f_{sat,i}$ is the hypothetical saturation fugacity of the penetrant and K_H is a function of parameters already defined (mainly polymer dependent).

All the quantities in the MFHE (eq 2) are fundamental and can potentially be estimated a priori (albeit with difficulty) and/or can be determined through diligent experimental efforts. An exception is a parameter in the quantity $f(s)$. It is an adjustable one that relates to the flexibility of the chains and currently can be only determined experimentally. We chose the MFHE model for our initial analysis because of the potential for relating its main parameters, ${}^{\infty}H_i$ and B_i, to mechanistic aspects of the sorption process in a fundamental way.

For completeness, the parameters of the dual-mode sorption (DMS) model[16,17] are also calculated and tabulated. The general form of this sorption model is

$$C_i = k_{D,i}f_i + C'_H bf_i/(1 + bf_i) \qquad (5)$$

where $k_{D,i}$ is the Henry's law solubility coefficient, C'_H is the Langmuir saturation capacity, and b is the Langmuir affinity constant. The DMS model intelligently combines two realistic population states (nonspecific and site specfic) for gas sorption, and the model's parameters are defined as physically satisfying quantities. It has been very successful in fitting the majority of experimental data for sorption in glassy polymers. This model is mostly empirical, and even though some limited success has been found in correlating its parameters with Lennard-Jones force constants and polymer glass transition temperatures,[18] they are not easily defined a priori by other fundamental properties.

The MFHE model was selected for our current work for several reasons: (1) it has fewer parameters, (2) its parameters can be further defined by more fundamental quantities that may facilitate the future development of predictive models, and (3) the MFHE model explicitly treats the effects of sorption-induced strain. This last point is especially significant following the theoretical treatment by Reiss et al.[19] They described the potential effect of spatial fluctuations in the mesoscopic-scale stress on the selectivity of gas-separating membranes. The inspiration for their work was the experimental evidence for steep stress gradients in PANi films fabricated for gas separations.

Table 1. Physical Properties of Penetrant Gases[a]

	critical temp, K	critical press., MPa	critical vol, cm^3/mol	liquid vol at NBP, cm^3/mol	12−6 σ, Å
Ar	150.8	4.874	74.9	29.1 (90 K)	3.542
O_2	154.6	5.046	73.4	27.8 (90 K)	3.467
N_2	126.2	3.394	89.5	34.8 (78 K)	3.798
He	5.2	0.227	57.3	32.5 (4.3 K)	2.551

[a] NBP = normal boiling point and 12−6 σ = Lennard−Jones collision diameter.

Results

To fit our experimental data with the MFHE model, we need to determine Φ_s (=Φ_i) in eq 2. We chose to use the solute's critical volume as its partial molar volume V_i (and we assume it stays constant) in the polymer's amorphous phase. An alternative choice is the liquid volume at the normal boiling point since gas sorption is presumed to proceed by a condensation mechanism. We hypothesized that gas sorption probably more closely represents the liquid- and gaslike state of a supercritical fluid and therefore chose the critical volume. The choice of the value for the solute's *constant* partial molar volume will affect the magnitude of the model parameters but not their trends. The polymer's amorphous volume fraction ϕ_a was set to 0.97 for the as-cast film and powder and 1 for the undoped film.[2] Other values of ϕ_a for PANi[20] are possible depending on processing conditions. Table 1 presents pertinent physical properties[21] of the penetrant gases used in this study. (He was used to measure sample volume.)

Figure 3 presents the sorption isotherms at 298 K for Ar, O_2, and N_2 in all the materials used in this study. The fitting lines were obtained using the MFHE model parameters. Table 2 presents the best fit for the parameters for the linear, MFHE, and DMS models. This table also contains the densities that were either measured (using the technique described in the Experimental/Apparatus Section) or reported in prior literature.[22] The parameters for the models were obtained using a fitting routine that was part of a commercial software program and was based on the Levenberg−Marquardt method. The DMS model fit was relatively insensitive to the value of the affinity constant b. Therefore, we set it equal to 0.001 Pa^{-1} for all the fits in order for the model to pass through the origin.

As-Cast PANi−Emeraldine Base Film. The fit to the O_2 sorption isotherm changes curvature as the pressure increases. More data, especially at higher pressures, are needed to confirm this behavior. The differences in overall sorption between Ar (and O_2) and N_2 are consistent with differences in "condensability" of those gases. This is often correlated with the critical temperature. The uncertainty limits on the B_i parameter are large; therefore, we can only make general comments about the trends. The difference in the B_i parameter between Ar and N_2 is consistent with the difference in their size, since the larger N_2 would cause more strain in sorption (thus making B_i more negative). The positive value of B_i for O_2 suggests a more complex effect from gas−polymer interaction potentials than we can currently explain. The positive value of B_i for O_2 sorption implies less strain or an easing of existing strain in this film as O_2 dissolves, perhaps due to plasticization. The DMS model's Henry's parameters

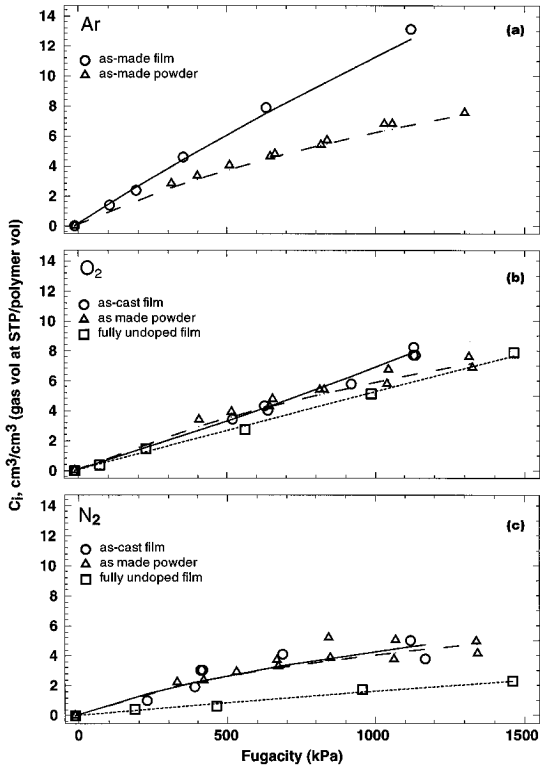

Figure 3. Direct comparison of sorption isotherms for (a) Ar, (b) O_2, and (c) N_2 in as-cast film, as-made powder, and fully undoped (cycled) film of PANi-EB (polyaniline emeraldine base) measured at 298 K. Curve fits are based on the modified Flory−Huggins model.

generally follow the gases' condensabilities and are comparable to the linear solubility fit.

As-Made PANi−Emeraldine Base Powder. This powder should represent the polymer without film-processing-induced morphological effects, such as extra free volume. The density of the EB powder was found to be 1.315 ± 0.023 g/cm^3 versus the 1.277 ± 0.028 g/cm^3 measured for the as-cast film. Even though these densities are equivalent within their uncertainties, the difference in the mean values is consistent with the presumption about less free volume in the powder. The isotherms for this material have the greatest curvature.

The B_i parameter becomes increasingly negative as the molecular size of the solute increases, and the sorption of all the test gases induces strain. There is very little measurable difference between O_2 and Ar, which is consistent with their similar sizes. All the solutes' B_i values are more negative in the powder than in the film. This trend is consistent with the powder being more dense than the film and probably developing more strain from solute sorption. The measured differences in the $^{\infty}H_i$ correlate with the critical temperature of the gas, thus reflecting the relative condensability of the solutes. The DMS model's k_D parameter (Henry's solubility) also decreases with increasing molecular size.

Undoped PANi−Emeraldine Base Film. In this case the difference between the sorption of O_2 and N_2 is much greater than in either the as-cast film or as-made powder—O_2 uptake is more than twice the N_2 value. This is primarily due to lower N_2 sorption. The isotherms are very linear, and there is very good agreement between the linear terms in the two models and the simple solubility parameter. The high uncertainty in the B_i parameter results because of this lack of curvature in the concentration against fugacity data within the range of our measurements. Notwithstanding this caveat, the B_i parameter is less negative for both components in this film than in the powder. The value for N_2 is more negative than that for O_2, which is consistent with the larger size of N_2. Also, since the undoped film has a lower density than the as-cast EB film, the B_i parameter for N_2 was less negative, suggesting less strain during sorption. But the O_2 had a more negative B_i in this cycled film than in the as-cast one, suggesting more strain. We will offer a rationale for this in the following discussion, where we consider structural insights from the X-ray diffraction studies.

Discussion

Maron et al.[2] studied the local molecular structure of amorphous PANi using a radial distribution function analysis of X-ray scattering data in combination with model calculations. Their results led to a (speculative) view of the local structure that provides a rationale for some of the observed sorption results. In general, they determined that as-cast EB films have poor interchain ordering relative to their intrachain structure; that is, the repeat unit segments do not regularly align to a significant degree. The process of "doping" tends to develop more regular bond angles in adjacent chains, due to the additions of the negative counterions (in their case Cl^-), causing the chain spacing to become more uniform; that is, some nearest neighbors along the chain get closer while others move apart. Undoping yields irreversible changes in the local interchain structure including larger gaps and smaller "pinch points" (volume constrictions). The net effect is an overall increase in free volume (supported by the measured decrease in density between as-cast and undoped films), but possibly more restricted access to it (that is, energy barriers or "bottlenecks").

Direct comparisons of the O_2 and N_2 sorption isotherms for the as-cast and undoped films (Figure 3b,c) indicate that there is little change in magnitude of the O_2 isotherm between these films. On the other hand, significantly less N_2 is absorbed in the undoped film than in the as-cast material. The decreased N_2 sorption in the undoped film supports the suggestion that the larger molecule has more difficulty accessing all the available free volume. The B_i parameters from the MFHE model indicated that more strain was induced by N_2 sorption in the as-cast film than in the undoped film. Our interpretation is that N_2 is completely excluded from more of the free volume in the undoped film than in the as-cast one. Therefore, N_2 mixes only with the polymer in the larger free volume regions—resulting in less induced strain. This is further supported by our observation that the Henry's solubility parameter is also lower in the undoped film.

As stated above, we perceive that there are free volume regions linked by "bottlenecks" in the PANi's microstructure. Although it produces "strain" in the polymer, the N_2 can diffuse through more of these restrictions in the as-cast film, thereby having access to additional sorption volume. In the undoped film more of the bottlenecks are absolute diffusion barriers to the N_2 within the time scale (days) of our measurements—therefore less strain in the polymer. The O_2 can still diffuse through many of bottlenecks in the undoped film, albeit at a slower rate; therefore, the equilibrium sorption capacity of the film for O_2 is roughly unchanged versus its value in the as-cast film.

Table 2. Parameters for Linear Solubility, MFHE, and DMS Sorption Models (298 K)

		MFHE		DMS[a]	
gas	$S = C/p$, $cm^3\ cm^{-3}\ Pa^{-1} \times 10^5$ (gas vol at STP)	${}^{\infty}H_i$, $cm^3\ cm^{-3}\ Pa^{-1} \times 10^5$ (gas vol at STP)	B_i	k_D, $cm^3\ cm^{-3}\ Pa^{-1} \times 10^5$ (gas vol at STP)	C'_H, $cm^3\ cm^{-3}$ (gas vol at STP)
	PANi-EB, As-Cast Film at 298 K (Density = 1.277 g/cm^3 ± 0.028)				
Ar	0.91 ± 0.02	1.01 ± 0.12	−6.8 ± 7.2	0.90 ± 0.05	0.13 ± 0.52
O_2	0.68 ± 0.01	0.61 ± 0.03	3.9 ± 2.2	0.74 ± 0.29	−0.56 ± 4.93
N_2	0.45 ± 0.05	0.80 ± 0.18	−45.7 ± 18.1	0.28 ± 0.22	1.21 ± 2.76
	PANi-EB, As-Made Powder at 298 K (Density = 1.315 g/cm^3 ± 0.023)				
Ar	0.65 ± 0.02	0.91 ± 0.04	−19.6 ± 2.6	0.50 ± 0.05	1.34 ± 0.68
O_2	0.60 ± 0.02	0.86 ± 0.07	−20.6 ± 4.1	0.42 ± 0.10	1.77 ± 1.72
N_2	0.42 ± 0.03	0.82 ± 0.13	−43.2 ± 10.8	0.24 ± 0.15	1.82 ± 2.34
	PANi-EB, Fully Undoped Film at 298 K (Density = 1.255[b] g/cm^3)				
O_2	0.52 ± 0.01	0.52 ± 0.02	−1.2 ± 2.0	0.52 ± 0.02	0.02 ± 0.26
N_2	0.16 ± 0.01	0.18 ± 0.01	−16.1 ± 10.1	0.16 ± 0.02	0.09 ± 0.30

[a] $b = 0.001\ Pa^{-1}$. [b] From ref 22.

The B_i values of the MFHE model suggest different mechanisms of O_2 sorption in the as-cast than in the undoped films, but it is difficult to argue that point too vigorously without more measurements especially at higher pressures. The possibility that O_2 can itself dope PANi is suggested by related literature.[23,24] If this were true, it would cause changes in local chain packing and free volume in as-cast films—an effect that could give rise to anomalous sorption due to concentration-dependent local relaxation. Even though the undoped film has greater free volume than the as-cast, oxygen's solubility is lower. This is probably due to hindered access to the available free volume.

Comparison of the various gases' sorption isotherms between the as-cast film and the as-made powder also focuses on effects from the available free volume in the polymer. Only Ar has a significantly higher sorption in the film than in the powder. An interpretation of the comparisons presented in Figure 3 is as follows:

(i) Nitrogen's sorption in both the film and the powder is in regions of similar energetics; the additional free volume created in the casting process is not energetically accessible to it.

(ii) Argon's smaller atomic size and greater condensability than nitrogen leads to its increased access to the extra free volume created in the cast film with a resulting higher solubility.

(iii) Oxygen's solubility in the powder is similar to the solubility of argon, indicating that the effects on solubility of their differences in size and critical temperature basically offset each other in the environment of the powder. At this point it is difficult to explain why oxygen does not have higher sorption in the as-cast film than we measured.

Conclusions

Oxygen's solubility in the as-cast film is higher than in the as-made powder or the undoped film. Nitrogen's solubilities in both the as-made powder and as-cast film were about the same and significantly greater than in the undoped film. In Table 3 we list the ideal O_2/N_2 solubility selectivity (ratio of pure component solubilities) as ∼1.8 for the as-cast film and 3.8 for the undoped.

Pure component permeation measurements on these films yield ideal O_2/N_2 selectivities (permeability ratios) of ∼7 for the as-cast film and ∼9 for the undoped one. The permeability difference for both species is lower in the undoped film, but the decrease is greater for N_2 than for O_2. From the above, the conventional conclusion is that the observed ideal O_2/N_2 separation factor in the as-cast film is primarily based on differences in diffusion coefficients, while in the undoped film solubility selectivity controls the permeability ratio. One could also argue that the solubility selectivity results from differences in diffusional access between the two films for the penetrants, and therefore diffusion controls the permselectivity in both films. We are continuing our measurements to further elucidate this hypothesis.

Table 3. Comparison between As-Cast and Fully Undoped PANi-EB Film

	as-cast film	undoped film
O_2 solubility[a]	8	6
N_2 solubility[a]	4.5	1.6
O_2/N_2 solubility selectivity	1.8	3.8
O_2 permeability[b]	0.265	0.146
N_2 permeability[b]	0.037	0.016
O_2/N_2 permeation selectivity	7.2	9.3
O_2/N_2 diffusivity selectivity[c]	4	2.4

[a] Nominal solubility, cm^3/cm^3 (gas vol at STP/polymer vol) at 1100 kPa and 298 K. [b] Permeability units ($cm^3\ cm\ cm^{-2}\ s^{-1}\ kPa^{-1}$) $\times 10^{10}$. [c] Calculated as equal to (permeation selectivity)/(solubility selectivity).

The MFHE model provided a consistent way to fit the experimental data with tighter confidence limits on most parameter estimates than for the DMS model.

The differences in solubility for the various combinations of the solute and form of PANi-EB can be attributed to the conventional physical properties of solute critical temperature and molecular size and accessible polymer free volume. Evidence was observed for a change in the accessible free volume of undoped versus as-cast PANi-EB film (dependent on the size of the solute). This supports a view that doping and undoping of PANi films can be used to create molecular size selective environments with respect to sorption as well as diffusion.

Acknowledgment. This work was funded in part by the DOE Advanced Industrial Materials (AIM) program, Office of Industrial Technology. J.P. and B.R.M. thank Shimshon Gottesfeld for many stimulating discussions.

Registry No. (provided by author). Ar, 7440-37-1; O_2, 7782-44-7; N_2, 7727-37-9; polyaniline, 25233-30-1; aniline [$C_6H_5NH_2$], 62-53-3; ammonium peroxydisulfate [$(NH_4)_2S_2O_8$], 7727-54-0; 1-methyl-2-pyrrolidinone [$(CH_3)NC_4H_6O$], 872-50-4; pyrrolidine [C_4H_9N], 123-75-1; ammonium hydroxide [NH_4OH], 1336-21-6; tetrahydro-

furan [C_4H_4O], 109-99-9; hydrochloric acid [HCl], 7647-01-0.

References and Notes

(1) Bitter, J. G. A *Transport Mechanisms in Membrane Separation Processes*; Plenum Press: New York, 1991.
(2) Maron, J.; Winokur, M. J.; Mattes, B. R. *Macromolecules* **1995**, *28*, 4475.
(3) Srinivasan, R.; Auvil, S. R.; Burban, P. M. *J. Membr. Sci.* **1994**, *86*, 67.
(4) Anderson, M. R.; Mattes, B. R.; Reiss, H.; Kaner, R. B. *Science* **1991**, *252*, 1412.
(5) Mattes, B. R.; Anderson, M. R.; Reiss, H.; Kaner, R. B. *Polym. Mater. Sci. Eng.* **1991**, *64*, 336.
(6) Mattes, B. R.; Anderson, M. R.; Reiss, H.; Kaner, R. B. In *Intrinsically Conducting Polymers: An Emerging Technology*; Aldissi, M., Ed.; NATO ASI Ser. E: Appl. Sci. Vol. 246; Kluwer Academic Publishers: Dordrecht, 1993; Chapter 7, p 61.
(7) Liang, W.; Martin, C. R. *Chem. Mater.* **1991**, *3*, 390.
(8) Kuwabata, S.; Martin, C. R. *J. Membr. Sci.* **1994**, *91*, 1.
(9) Koros, W. J.; Paul, D. R. *J. Polym. Sci., Polym. Phys. Ed.* **1976**, *14*, 1903.
(10) Felder, R. M.; Huvard, G. S. In *Methods of Experimental Physics*; Fava, R. A., Ed.; Academic Press: New York, 1980; Vol. 16C, Chapter 17, p 315.
(11) Younglove, B. A. *J. Phys.Chem. Ref. Data* **1982**, *11* (Suppl. 1).
(12) Friend, D. G.; Huber, M. L. *Int. J. Thermophys.* **1994**, *15*, 1279.
(13) Wei, Y.; Jang, G.-Y.; Hsueh, K. F.; Scherr, E. M.; MacDiarmid, A. G.; Epstein, A. J. *Polymer* **1992**, *33*, 314.
(14) Raucher, D.; Sefcik, M. D. In *Industrial Gas Separations*; Whyte, T. E., Yon, C. M., Wagener, E. H., Eds.; ACS Symp. Ser. No. 223; American Chemical Society: Washington, DC, 1983; Chapter 6, p 111.
(15) The notation cm^3 [STP] means volume measured at standard temperature and pressure, 273.15 K and 101.83 kPa.
(16) Koros, W. J.; Chan, A. H.; Paul, D. R. *J. Membr. Sci.* **1977**, *2*, 165.
(17) Michaels, A. S.; Vieth, W. R.; Barrie, J. A. *J. Appl. Phys.* **1963**, *34*, 1.
(18) Petropoulos, J. H. In *Polymeric Gas Separation Membranes*; Paul, D. R., Yampol'skii, Y. P., Eds.; CRC Press. Boca Raton, FL, 1994; Chapter 2, p 17.
(19) Reiss, H.; Anderson, M. R.; Murphy, W. D. *J. Membr. Sci.* **1994**, *88*, 145.
(20) Pouget, J. P.; Jozefowicz, M. E.; Epstein, A. J.; Tang, X.; MacDiarmid, A. G. *Macromolecules* **1991**, *24*, 779.
(21) Reid, R. C.; Prausnitz, J. M.; Sherwood, T. K. *The Properties of Gases and Liquids*, 3rd ed.; McGraw-Hill: New York, 1977.
(22) Mattes, B. R. PhD Dissertation, University of California—Los Angeles, Los Angeles, CA, 1992.
(23) Hanawa, T.; Yoneyma, H. *Synth. Met.* **1989**, *30*, 341.
(24) Calleja, R. D.; Maveeva, E. S. *J. Phys. (Paris)* **1993**, IV, 3, C7, 1569.

MA951333X